Hindawi Publishing Corporation
ISRN Nanomaterials
Volume 2013, Article ID 745397, 7 pages
http://dx.doi.org/10.1155/2013/745397

Research Article

Mesoporous SiO_2-Supported Pt Nanoparticles for Catalytic Application

Yingze Cao, Wentao Zhai, Xiang Zhang, Shuxi Li, Lin Feng, and Yen Wei

Department of Chemistry, Tsinghua University, Beijing 100084, China

Correspondence should be addressed to Lin Feng; fl@mail.tsinghua.edu.cn and Yen Wei; weiyen@tsinghua.edu.cn

Received 4 December 2012; Accepted 30 December 2012

Academic Editors: C. Angeles-Chavez, A. Fidalgo, M. Mirzaei, and A. V. Raghu

SiO_2 nanoparticles have been synthesized by combining Stober's method and nonsurfactant process. The diameters and pore sizes can be controlled by altering the template and its concentration. Mesoporous SiO_2 obtained this way has extremely large surface area compared with most oxide supports, which benefits the catalytic performance. Pt nanoparticles were in situ grown on and in mesoporous SiO_2 nanoparticles with low amount of the metal and high load ratio. Furthermore, we firstly developed a novel route, called "one-pot" method, to prepare Pt/SiO_2 catalyst where mesoporous silica preparing and Pt loading occurred in one step. This method is more efficient in saving reagent, since it can prevent Pt loss. In the meantime, it enables the template to reduce agent. The catalytic activity of Pt/SiO_2 samples was measured by CO oxidation. It is indicated that the supporting silica with mesopores is more active than silica with micropores.

1. Introduction

With the acceleration of industrialization and the increase of pollution, new catalysts development becomes very important. It is especially true when it comes to catalysts used to process gases from the incomplete combustion [1]. The incomplete combustion occurs in gasoline engine mainly discharges three kinds of harmful emissions: carbon monoxide (CO), unburned hydrocarbon emissions, and nitrogen oxides (NOx) [2]. With the establishment of stricter exhaust standards, together with the limit reserves and high cost of rare metals, preparing efficient catalyst with trace rare metals becomes the focus of study [3].

Three-way catalysis (TWC) which is a revolution can simultaneously converse the three major emissions into CO_2, H_2O, and N_2. The active substance of TWC is usually made of Pt, Pd, and Rh loaded on oxide supporting [2]. Recently, many researches have been developed around oxide supporting such as ceria, zirconia, alumina, and composite ceria-zirconia supporting [4–11]. Silica has also been used for supporting noble metals. For example, mixed oxide catalysts silica-ceria have been prepared through coprecipitation after hydrothermal synthesis for reduction and oxygen storage. The noble metals were loaded after calcination of the supports. The catalyst was fairly active. The full CO oxidation conversion was about 400°C, and the calcination limited the oxygen storage [12]. Also the catalytic performances of noble metals supported on mesoporous silica MCM-41 were investigated for the hydrodesulfurization of benzothiophene. MCM-41 was made by the surfactant method and had been treated at a very high temperature to remove the template. The catalytic reaction was carried out at 350°C which is quite high [13].

Silica is low-priced and easy to synthesize [14]. So far, most mesoporous materials are using ionic or neutral surfactants as templates to form the mesopores [15–21]. In some conditions, the species of surfactants have a number of drawbacks. For example, some cationic surfactants are toxic and expensive. The synthesis and template-removal process with surfactant method is often under harsh conditions such as high temperature and pressure and strongly acidic or alkaline media which could harm the catalyzer that the mesoporous material loads. Recent reports have shown that surfactants have side effects on the catalysis of metallic nanoparticle [22]. To solve these problems, since 1988, our group has been working on devising a novel nonsurfactant sol-gel process to make mesoporous silica materials [23–26]. This method employs small and mild molecules as templates which can be simply removed by water extraction. The pore

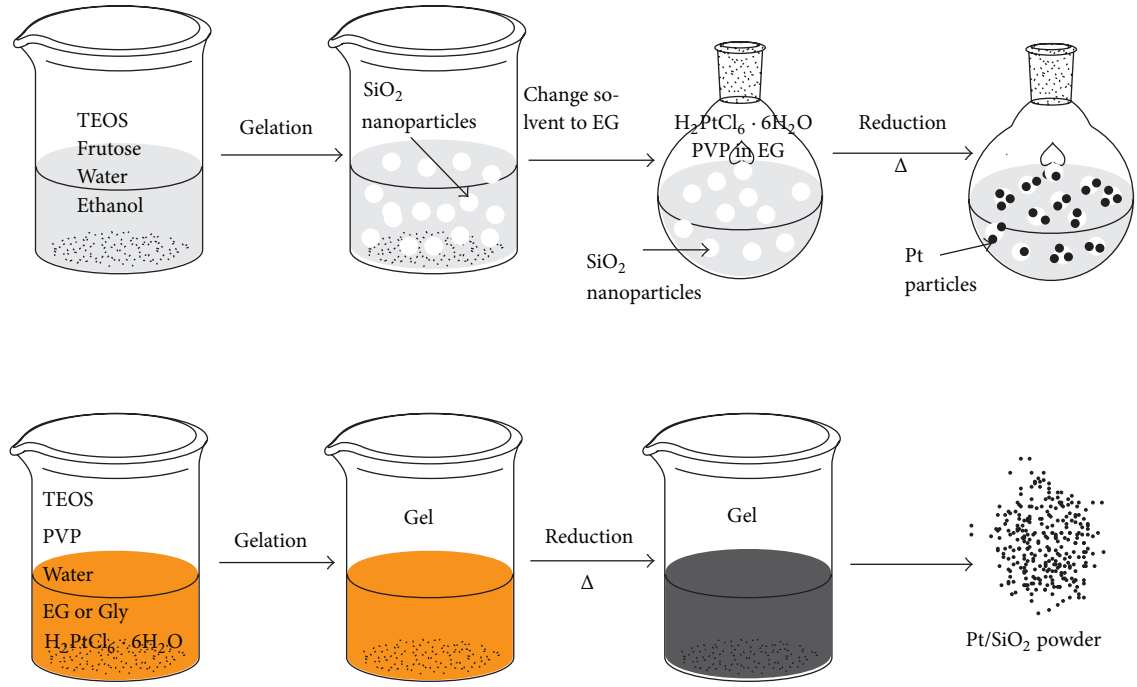

Figure 1: Schematic diagram of the synthetic process of Pt/SiO_2 catalysts in two different ways, two stages (above) for preparation of Pt on SiO_2 nanoparticles while only one (below) in the "one-pot" preparation of Pt/SiO_2.

diameter of nonsurfactant mesoporous silica is narrowly distributed and tunable (2~12 nm) which can be achieved by altering the template and its concentration. In 2009, we successfully synthesized mesoporous silica nanoparticles by combining Stober's method and nonsurfactant process [27].

Herein, we made an attempt to prepare Pt loaded mesoporous silica catalysts using two different ways. Firstly, loading Pt nanoparticles on silica nanoparticles by reduction of Pt containing salt, mesopores gives a novel triple-nanostructural catalytic material. At low ratio of $Pt:SiO_2$, the catalytic activity of CO oxidation supported by mesoporous silica is much better than SiO_2 nanoparticles with micropores. Another attempt was to combine monolithic mesoporous silica preparation and Pt load in one step which is more convenient and Pt economical. In the "one-pot" method the template for mesopores silica is also used for reduction of Pt. Similarly, Pt/SiO_2 with mesopores has much better activity of CO oxidation than those with micropores. This further confirms that Pt/SiO_2 catalyst with mesopores have higher activity than that with micropores.

2. Experimental Section

2.1. Chemicals. Chloroplatinic acid was purchased from Alfa Aesar, and all other chemicals were purchased from Sinopharm Chemical Reagent Co., Ltd. The water used in all experiments was deionized water. All the chemicals were of analytical grade and used as received without further purification.

2.2. Preparation of Pt on SiO_2 Nanoparticles. For the preparation of SiO_2 nanoparticles, a typical procedure described in [27] was used. The SiO_2 nanoparticles were synthesized by using fructose as template. 100 and 1000 nm diameters of SiO_2 nanoparticles were designated as samples NP-100 and NP-1000, respectively. Both were dried out for further use.

In a typical procedure, 40 mL deionized water contained 0.1 g SiO_2 nanoparticles, 0.038 g $H_2PtCl_6 \cdot 6H_2O$, 0.055 g PVP (MW = 55000 g/mol) and 10 mL ethylene glycol was mixed and ultrasonic-treated at room temperature. After 10-minute vigorous agitation, the solution was transferred into a silicone oil bath kept at 110°C until the solution got dark brown. The container was taken out after 5 minutes. Then it was naturally cooled down to room temperature. The solution was separated nearly equally into two centrifuge 50 mL tubes and centrifuged at 7000 r/min for 15 minutes. The precipitate at the bottom were washed both by deionized water and absolute ethanol three times and then dried out in a drying oven at 60°C overnight for further research. The Pt loaded samples were designated as NP-100-Pt and NP-1000-Pt. Samples 1/10-NP-100-Pt and 1/10-NP-1000-Pt were obtained by cutting down the Pt precursor ratio to 1/10. All the procedures can be simply described as two stages showed in Figure 1.

2.3. "One-Pot" Preparation of Pt/SiO_2. The encapsulation of chloroplatinic acid was achieved by hydrolysis and polycondensation, that is, sol-gel reactions of tetraethyl orthosilicate (TEOS) in the presence of ethylene glycol as the nonsurfactant template as well as reductive agent at room temperature

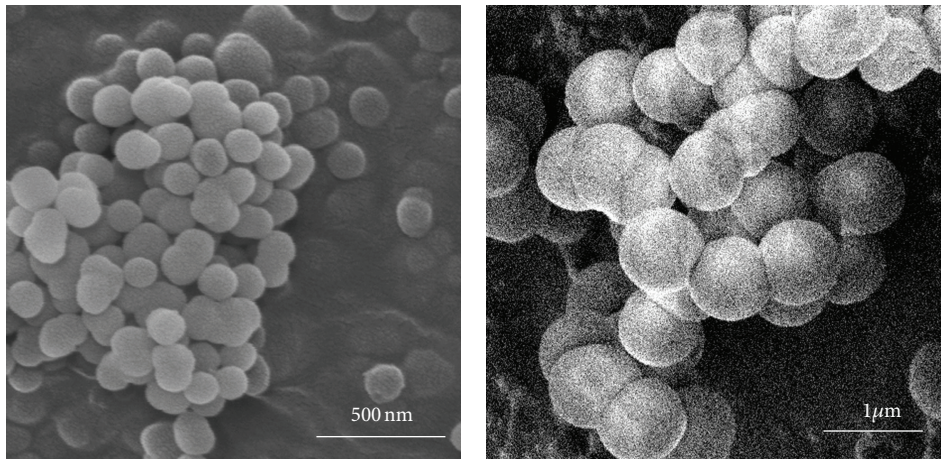

(a) (b)

Figure 2: (a) SEM image of as-prepared SiO_2 nanoparticles with a narrow distributed size of about 100 nm in diameter. (b) SEM image of SiO_2 nanoparticles with a fairly narrow distribution of sizes around 1000 nm in diameter.

[28]. 4.0 g TEOS was hydrolyzed by 1 mL 0.17 mol/L HCl in a 100 mL beaker. 0.038 g $H_2PtCl_6 \cdot 6H_2O$, 0.055 g PVP (MW = 55000 g/mol) and 0.69 g ethylene glycol were added after the hydrolysis. The solution, sealed by plastic film, was stirred at room temperature for 3 days to become a yellow gel.

The gel without any treatment was taken to a drying oven at 110°C for about 1 hour. The gel went dark brown, and it cracked into smaller pieces. These pieces were crushed into fine powder. Then the powder was washed by deionized water and absolute ethanol three times. At last the washed powder was dried out in a drying oven at 60°C overnight for further research. With the same procedure glycerol template SiO_2 has been made as well as the control sample without Pt precursor. The procedures are also shown in Figure 1 which all occurred in one beaker.

2.4. Characterizations. The size and morphology of the SiO_2 nanoparticles were determined by a PF3950/00 scanning electron microscopy (SEM). Transmission electron microscope (TEM) was carried out using a JEM-1200 EX transmission electron microscope instrument. The N_2 sorption characterization on the powdered samples was conducted on a Micromeritics ASAP 2010 Surface Area and Pore-Size Analyzer (Micromeritics, Norcross, GA) at −196°C in liquid nitrogen. The samples were degassed at 200°C and 10^{-6} Torr for several hours prior to N_2 adsorption-desorption measurement. Energy dispersive X-ray analysis (EDXA) was performed on a Sirion 200 scanning electron microscope equipped with an EDXA system to acquire the platinum content of the catalyst. The catalytic activities for CO oxidation were evaluated in a fixed-bed quartz tubular reactor. The catalyst particles (0.2 g) were placed in the reactor. The gas reactant (1.0% CO, 16% O_2, balanced with nitrogen) went through the reactor at 100 mL/min. The composition of the gas exiting the reactor was monitored by gas chromatography equipped with a hydrogen flame ionization detector and a TDX column. Reaction temperature was controlled by a thermocouple adjustable from room temperature to 700°C. Temperature needed for 100% CO conversion was defined as the criteria for the activity of catalysts.

3. Results and Discussion

3.1. SiO_2 Nanoparticles Support Pt Catalysts. Typical scanning electron microscopy (SEM) images obtained for SiO_2 nanoparticles are shown in Figure 2. Figure 2(a) shows SEM image of as-prepared SiO_2 nanoparticles with a narrow distributed size of about 100 nm in diameter. Figure 2(b) shows SEM image of SiO_2 nanoparticles with a fairly narrow distribution of sizes around 1000 nm in diameter. These two different kinds of SiO_2 nanoparticles are well uniformly structured but some adhesions can be seen in the image. In the synthesis of SiO_2 nanoparticles, the diameter of SiO_2 nanoparticles and pore size are simultaneously determined by the amount of template, fructose in this case. The sample was washed by abundant water till the filtrate was nearly neutral to remove the fructose template and ammonia before the characterization with isothermal N_2 adsorption-desorption. Brunauer-Emmett-Teller (BET) surface area and k pore parameters are summarized in Table 1. Figure 3 shows N_2 adsorption-desorption isotherms at various relative pressure (P/P_0 = 0–1) of the samples NP-100 and NP-1000. The results indicate that NP-100 which was made by less fructose template is essentially microporous which has quite small pore size and volume. The N_2 adsorption-desorption isotherm of NP-100 sample has no hysteresis loop which is type I isotherm while NP-1000 sample with more fructose templates shows typical IV-like isotherms with H2 hysteresis loops according to IUPAC [29]. The H2 hysteresis loop represents the pores of the sample which are mainly mesopores. This can be further certified by BJH pore distributions in electronic Supplementary Material available online at http://dx.doi.org/10.1155/2013/745397. NP-1000 sample with 80% (w/w) template has a narrow distributed diameter centering at 3.3 nm.

Table 1: BET surface, BJH pore size, and pore volume of all samples after the removal of different templates, and the effect of the catalytic activity of Pt/SiO_2 catalysts.

Sample code	Template	S_{BET} (m^2/g)	V_SP (cm^3/g)	BJH pore size (nm)	$T100\%$ (°C)
NP-100	Fructose	540	0.25	2.2	—
NP-1000		710	0.53	3.3	—
NP-100-Pt		103	0.1	—	130
NP-1000-Pt		614	0.43	3.2	130
EG	Ethylene glycol	479	0.54	4.1	—
Gly	Glycerol	557	0.32	3.3	—
EG-Pt	Ethylene glycol	580	0.37	3.8	150
Gly-Pt	Glycerol	772	0.39	2.5	220

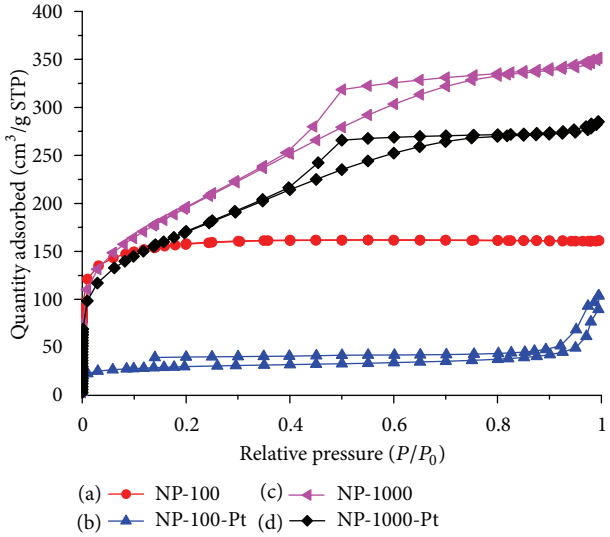

Figure 3: N_2 adsorption-desorption isotherms of different size of SiO_2 nanoparticles before and after loading Pt nanoparticles on (a) NP-100, (b) NP-100-Pt, (c) NP-1000, and (d) NP-1000-Pt. The results indicate that NP-100 which was made by less fructose template is essentially microporous which can be blocked by Pt. N_2 adsorption-desorption isotherms (c) and (d) show that NP-1000 and NP-1000-Pt are mainly mesoporous even after Pt loading. Mesoporous SiO_2 support leads faster gas flow than microporous support to thus mesoporous Pt/SiO_2 have much better activity.

Figures 4(a) and 4(b) illustrate transmission electron microscope (TEM) images of sample NP-100 before (a) and after (b) loading Pt nanoparticles, showing NP-100 with a narrow distribution of diameter around 100 nm and Pt nanoparticles as small dark spots. It confirmed that Pt nanoparticles had been well deposited on and in SiO_2 nanoparticles. Pt whose size is 2 to 3 nm in diameter was well dispersed. BET results of NP-100-Pt and NP-1000-Pt can also be seen in Figures 3(c) and 3(d). After the loading, the BET surface area of NP-100-Pt decreases beyond 80% (from 540 to 103 m^2/g) while only decreases by 14% for NP-1000-Pt (from 710 to 614 m^2/g). BJH pore size shown in Figure 3 illustrates that the pores of NP-100-Pt are blocked out by Pt nanoparticles while pores of NP-1000 are not. It leads to the big differences of the BET surface area reduction. Catalysts with large surface area provide more reaction sites between Pt and the exhaust gas to improve the catalytic activity. Energy dispersive X-ray analysis (EDXA) results in the electronic Supplementary Material further confirmed that there are only Si, O, and Pt existing in the as-prepared NP-1000-Pt.

3.2. "One-Pot" Method of Preparation Pt/SiO_2. "One-pot" method for preparation of Pt/SiO_2 adopted the same ratio of 1/10-NP-1000-Pt. Figure 5 shows the TEM image of sample prepared by "one-pot" method after removing ethylene glycol template. Pt nanoparticles as small black spots in the TEM image show that chloroplatinic acid was encapsulated before gelation and then reduced in situ. There is no Pt loss in this method. Ethylene glycol is reductant as well as template. All BET surface areas and pore sizes are also summarized in Table 1. Figures 6(a) and 6(c) show N_2 adsorption-desorption isotherms of the ethylene glycol template samples with (c) and without (a) encapsulating chloroplatinic acid. Both are type IV-like isotherms with type H2 hysteresis loops that represent mesopores which are mainly in the samples, while glycerol template sample has no loops in the N_2 adsorption-desorption isotherm in Figures 6(b) and 6(d) which indicates that the pores are mainly mircopores.

3.3. Catalysts for CO Oxidation. The catalytic activity for CO oxidation of NP-100-Pt and NP-1000-Pt was tested from low conversion to 100% conversion. Figures 7(a) and 7(b) show these two kinds of Pt/SiO_2 nanoparticles with higher ratio of chloroplatinic acid and SiO_2 nanoparticles nearly have the similar full CO conversion temperature, around 130°C. Figure 7(d) shows that the 1/10-NP-1000-Pt remains well in activity when the temperature of full CO conversion is about 140°C while the 1/10-NP-100-Pt has more drops in activity according to Figure 7(c). This huge difference is highly possible caused by pore size on SiO_2 nanoparticles. The lower ratio Pt/SiO_2 nanoparticles with mesoporous SiO_2 support are satisfied compared to some other oxide supports considering the activity, cost, environmental-friendly preparation conditions, and the difficulty of preparation. Thus it makes a good catalyst for industrial application.

With the same low ratio, Figures 7(d) and 7(e) show that ethylene glycol template Pt/SiO_2 (EG-Pt) keep up the activity (full CO conversion temperature is 150°C) compared

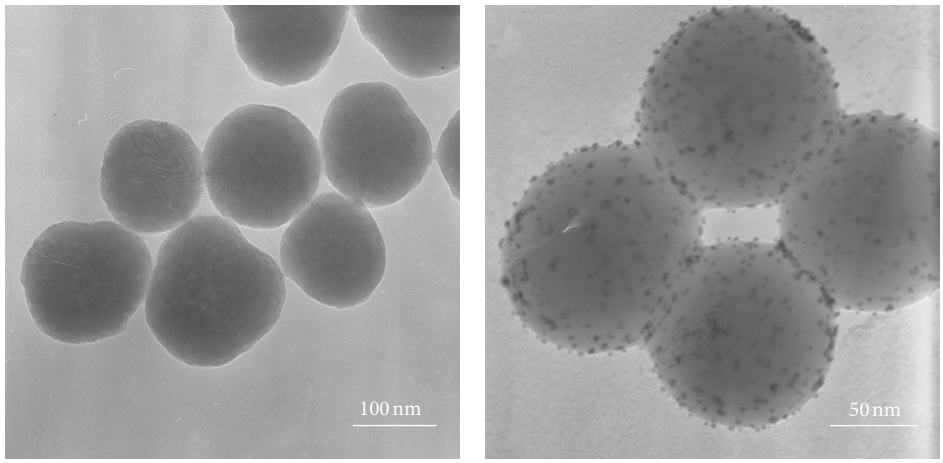

(a) (b)

Figure 4: TEM images of sample NP-100 before (a) and after (b) loading Pt nanoparticles, showing NP-100 with a narrow distribution of diameter around 100 nm and Pt nanoparticles as small dark spots. Pt nanoparticles whose size is 2 to 3 nm in diameter were well dispersed.

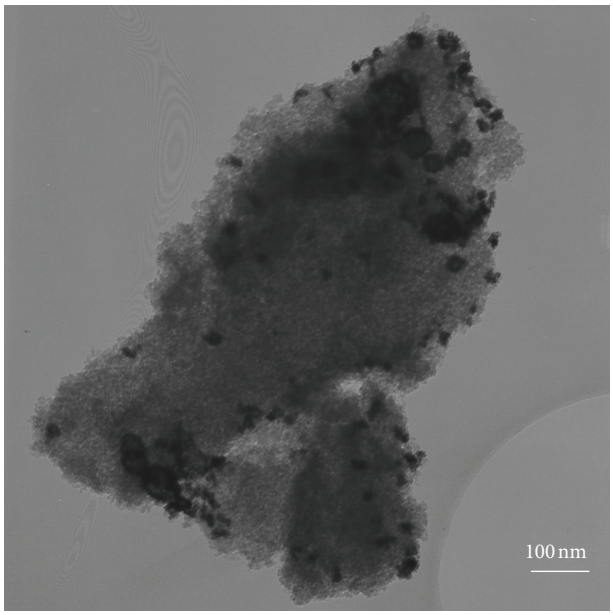

Figure 5: TEM image of Pt/SiO_2 prepared by "one-pot" method with ethylene glycol as template. Pt nanoparticles as small black spots in the TEM image show that chloroplatinic acid was encapsulated before gelation and then reduced in situ. There is no Pt loss in this method.

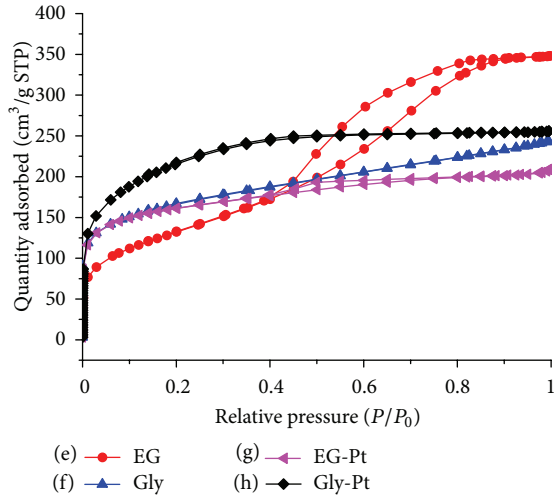

Figure 6: N_2 adsorption-desorption isotherms of "one-pot" method for prepared Pt/SiO_2 after removal of templates and the controlled samples: (e) EG, (f) Gly, (g) EG-Pt, and (h) Gly-Pt. (e) and (g) are type IV-like isotherms with type H2 hysteresis loops that represents mesopores which are mainly in the samples, while glycerol template sample has no loops in the N_2 adsorption-desorption isotherm (b) and (d) which indicates that the pores are mainly mircopores.

to 1/10-N-1000-Pt, while the catalytic activity of glycerol template Pt/SiO_2 (Gly-Pt) descend a lot (full CO conversion temperature is 220°C). This huge difference may be the result of the different pore size of the silica materials. As is known to all, gas can diffuse more quickly and freely through SiO_2 with mesopores than micropores [30]. Thus CO has more chances to be oxidated by Pt. The oxidation product CO_2 is much easier to get away from the catalyst with mesopores. In conclusion, Pt/SiO_2 catalyst has better activity with mesopores than micropores.

4. Conclusion

In summary, we successfully synthesized Pt/SiO_2 catalyst with different kinds of silica supporting which has quite large BET surface area. At high ratio of $Pt:SiO_2$, the catalytic activity of CO oxidation showed no difference between SiO_2 nanoparticles with mesopores and mircopores (full CO conversion temperature is 130°C). When the ratio decreased to 1/10, the activity of the Pt/SiO2 catalyst can almost remain when supported by the mesoporous silica but that has a great drop when supported by the microporous one. In the "one-pot" method with two kinds of template and same lower ratio,

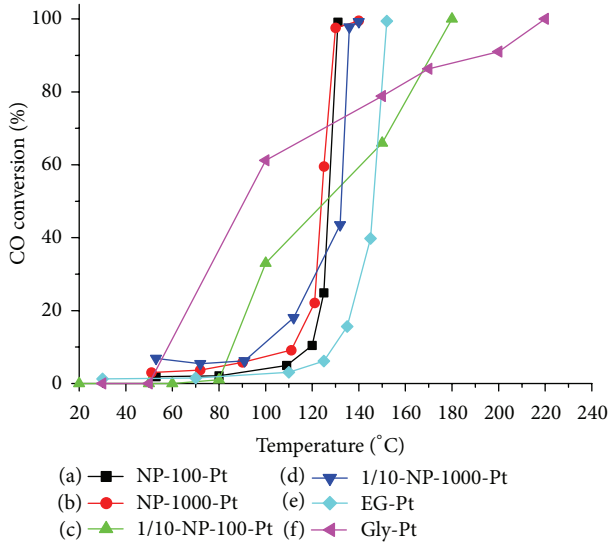

FIGURE 7: Catalytic performance of as-prepared Pt/SiO_2 samples with different templates by different methods: (a) NP-100-Pt, (b) NP-1000-Pt, (c) 1/10-NP-100-Pt, (d) 1/10-NP-1000-Pt, (e) EG-Pt, and (f) Gly-Pt. At low ratio mesoporous Pt/SiO_2 catalysts prepared by both methods (d) and (e) have better activity than microporous Pt/SiO_2 (c) and (f).

ethylene glycol template Pt/SiO_2 have much better activity of CO oxidation than glycerol. The temperature of full CO conversion of EG-Pt is 150°C while Gly-Pt is 220°C. The pore sizes of silica can be altered by different templates; that is, mesopores can be obtained with ethylene glycol while micropores with glycerol. This further confirmed that Pt/SiO_2 catalyst has higher activity with mesopores than micropores. The mesopores SiO_2-supported Pt catalysts are potentially applied for gas purification especially for harmful emissions from automobile.

Acknowledgments

The authors thank the project funded by the National Natural Science Foundation of China under Grants nos. 20921001, 51173099, 21134004 and the National Key Basic Research and Development Program of China under Grant no. 2011CB935700. They thank Professor. Weiguo Song (Institute of Chemistry, Chinese Academy of Sciences) and Professor. Yadong Li (Tsinghua University) for catalyst evaluation.

References

[1] Q. Wang, G. Li, B. Zhao, and R. Zhou, "Investigation on properties of a novel ceria-zirconia-praseodymia solid solution and its application in Pd-only three-way catalyst for gasoline engine emission control," *Fuel*, vol. 90, no. 10, pp. 3047–3055, 2011.

[2] S. Bernal, G. Blanco, J. J. Calvino, J. M. Gatica, J. A. P. Omil, and J. M. Pintado, "Characterisation of three-way automotive aftertreatment catalysts and related model systems," *Topics in Catalysis*, vol. 28, no. 1–4, pp. 31–46, 2004.

[3] H. Birgersson, L. Eriksson, M. Boutonnet, and S. G. Jaras, "Thermal gas treatment to regenerate spent automotive three-way exhaust gas catalysts (TWC)," *Applied Catalysis B*, vol. 54, no. 3, pp. 193–200, 2004.

[4] L. Feng, D. T. Hoang, C. K. Tsung et al., "Catalytic properties of Pt cluster-decorated CeO_2 nanostructures," *Nano Research*, vol. 4, no. 1, pp. 61–71, 2011.

[5] A. Iglesias-Juez, A. B. Hungria, A. Martinez-Arias, J. A. Anderson, and M. Fernandez-Garcia, "Pd-based (Ce,Zr)O*x*-supported catalysts: promoting effect of base metals (Cr, Cu, Ni) in CO and NO elimination," *Catalysis Today*, vol. 143, no. 3-4, pp. 195–202, 2009.

[6] I. Heo, J. W. Choung, P. S. Kim et al., "The alteration of the performance of field-aged Pd-based TWCs towards CO and C_3H_6 oxidation," *Applied Catalysis B*, vol. 92, no. 1-2, pp. 114–125, 2009.

[7] H. Linhua, S. Keqiang, P. Qing, X. Boqing, and L. Yadong, "Surface active sites on Co_3O_4 nanobelt and nanocube model catalysts for CO oxidation," *Nano Research*, vol. 3, no. 5, pp. 363–368, 2010.

[8] H. Noei, S. Amirjalayer, M. Muller et al., "Low-Temperature CO oxidation over Cu-based metal-organic frameworks monitored by using FTIR spectroscopy," *ChemCatChem*, vol. 4, no. 6, pp. 755–759, 2012.

[9] O. Metin, S. Ozkar, and S. Sun, "Monodisperse nickel nanoparticles supported on SiO_2 as an effective catalyst for the hydrolysis of ammonia-borane," *Nano Research*, vol. 3, no. 9, pp. 676–684, 2010.

[10] A. Suda, K. Yamamura, A. Morikawa et al., "Atmospheric pressure solvothermal synthesis of ceria-zirconia solid solutions and their large oxygen storage capacity," *Journal of Materials Science*, vol. 43, no. 7, pp. 2258–2262, 2008.

[11] X. Wang, G. Lu, Y. Guo, L. Jiang, Y. Guo, and C. Li, "Effect of additives on the structure characteristics, thermal stability, reducibility and catalytic activity of CeO_2-ZrO_2 solid solution for methane combustion," *Journal of Materials Science*, vol. 44, no. 5, pp. 1294–1301, 2009.

[12] B. M. Reddy, A. Khan, P. Lakshmanan, M. Aouine, S. Loridant, and J. C. Volta, "Structural characterization of nanosized CeO_2-SiO_2, CeO_2-TiO_2, and CeO_2-ZrO_2 catalysts by XRD, Raman, and HREM techniques," *Journal of Physical Chemistry B*, vol. 109, no. 8, pp. 3355–3363, 2005.

[13] Y. Kanda, A. Seino, T. Kobayashi, Y. Uemichi, and M. Sugioka, "Catalytic performance of noble metals supported on mesoporous silica MCM-41 for hydrodesulfurization of benzothiophene," *Journal of the Japan Petroleum Institute*, vol. 52, no. 2, pp. 42–50, 2009.

[14] E. Rocchini, M. Vicario, J. Llorca, C. de Leitenburg, G. Dolcetti, and A. Trovarelli, "Reduction and oxygen storage behavior of noble metals supported on silica-doped ceria," *Journal of Catalysis*, vol. 211, no. 2, pp. 407–421, 2002.

[15] C. T. Kresge, M. E. Leonowicz, W. J. Roth, J. C. Vartuli, and J. S. Beck, "Ordered mesoporous molecular sieves synthesized by a liquid-crystal template mechanism," *Nature*, vol. 359, no. 6397, pp. 710–712, 1992.

[16] J. Y. Ying, C. P. Mehnert, and M. S. Wong, "Synthesis and applications of supramolecular-templated mesoporous materials," *Angewandte Chemie*, vol. 38, no. 1-2, pp. 57–77, 1999.

[17] N.-B. Zhang, J.-J. Xu, and C.-G. Xue, "Core-shell structured mesoporous silica nanoparticles equipped with pyrene-based chemosensor: synthesis, characterization, and sensing activity

towards Hg(II)," *Journal of Luminescence*, vol. 131, no. 9, pp. 2021–2025, 2011.

[18] C. Morelli, P. Maris, D. Sisci et al., "PEG-templated mesoporous silica nanoparticles exclusively target cancer cells," *Nanoscale*, vol. 3, no. 8, pp. 3198–3207, 2011.

[19] J. Zhang, X. Li, J. M. Rosenholm, and H.-C. Gu, "Synthesis and characterization of pore size-tunable magnetic mesoporous silica nanoparticles," *Journal of Colloid and Interface Science*, vol. 361, no. 1, pp. 16–24, 2011.

[20] X.-J. Wu, Y. Jiang, and D. Xu, "A unique transformation route for synthesis of rodlike hollow mesoporous silica particles," *Journal of Physical Chemistry C*, vol. 115, no. 23, pp. 11342–11347, 2011.

[21] L. Du, S. Liao, Q. Liu et al., "Porous grape-like spherical silica with hydrogen storage capability, synthesized using neutral dual surfactants as templates," *International Journal of Hydrogen Energy*, vol. 34, no. 9, pp. 3810–3815, 2009.

[22] U. P. Azad, V. Ganesan, and M. Pal, "Catalytic reduction of organic dyes at gold nanoparticles impregnated silica materials: influence of functional groups and surfactants," *Journal of Nanoparticle Research*, vol. 13, no. 9, pp. 3951–3959, 2011.

[23] Y. Wei, D. Jin, T. Ding et al., "A non-surfactant templating route to mesoporous silica materials," *Advanced Materials*, vol. 10, no. 4, pp. 313–316, 1998.

[24] J. B. Pang, K. Y. Qiu, Y. Wei, X. J. Lei, and Z. F. Liu, "A facile preparation of transparent and monolithic mesoporous silica materials," *Chemical Communications*, no. 6, pp. 477–478, 2000.

[25] J. B. Pang, K. Y. Qiu, and Y. Wei, "Preparation of mesoporous silica materials with non-surfactant hydroxy-carboxylic acid compounds as templates via sol-gel process," *Journal of Non-Crystalline Solids*, vol. 283, no. 1–3, pp. 101–108, 2001.

[26] J. Y. Zheng, J. B. Pang, K. Y. Qiu, and Y. Wei, "Synthesis and characterization of mesoporous titania and silica-titania materials by urea templated sol-gel reactions," *Microporous and Mesoporous Materials*, vol. 49, no. 1–3, pp. 189–195, 2001.

[27] I. Mukherjee, A. Mylonakis, Y. Guo et al., "Effect of nonsurfactant template content on the particle size and surface area of monodisperse mesoporous silica nanospheres," *Microporous and Mesoporous Materials*, vol. 122, no. 1–3, pp. 168–174, 2009.

[28] Y. Wei, J. Xu, Q. Feng, H. Dong, and M. Lin, "Encapsulation of enzymes in mesoporous host materials via the nonsurfactant-templated sol-gel process," *Materials Letters*, vol. 44, no. 1, pp. 6–11, 2000.

[29] K. S. W. Sing, D. H. Everett, R. A. W. Haul et al., "Reporting physisorption data for gas/solid systems with special reference to the determination of surface area and porosity (Recommendations 1984)," *Pure and Applied Chemistry*, vol. 57, no. 4, pp. 603–619, 1985.

[30] B. Hosticka, P. M. Norris, J. S. Brenizer, and C. E. Daitch, "Gas flow through aerogels," *Journal of Non-Crystalline Solids*, vol. 225, no. 1–3, pp. 293–297, 1998.